Nuclear energy density functionals for astrophysics (and nuclear physics)

Nicolas Chamel
in collaboration with S. Goriely and J. M. Pearson

Institute of Astronomy and Astrophysics
Université Libre de Bruxelles, Belgium

YIPQS, Kyoto, 22 September 2011

Outline

1. Nuclear energy density functional
   - theory
   - pairing
   - spin-isospin instabilities
   - self-interactions
   - neutron-matter stiffness

2. Applications to neutron stars
   - unified equation of state for crust and core
   - global structure

Why do we need functionals for astrophysics?

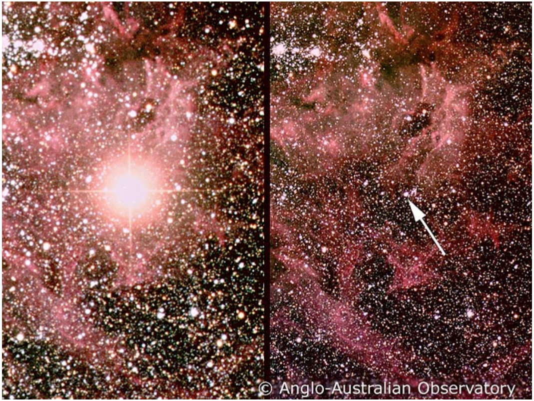

The interpretation of many astrophysical phenomena requires the knowledge of nuclear properties which are not experimentally accessible and won't be measured in a near future

Nuclear energy density functional theory in a nut shell

The nuclear energy density functional theory allows for a **tractable and consistent** treatment of various nuclear systems from atomic nuclei to neutron stars.

The energy of a lump of matter is expressed as ($q = n, p$)

$$E = \int \mathcal{E}\Big[\rho_q(\boldsymbol{r}), \boldsymbol{\nabla}\rho_q(\boldsymbol{r}), \tau_q(\boldsymbol{r}), \boldsymbol{J}_q(\boldsymbol{r}), \tilde{\rho}_q(\boldsymbol{r})\Big]\, \mathrm{d}^3\boldsymbol{r}$$

where $\rho_q(\boldsymbol{r})$, $\tau_q(\boldsymbol{r})$... are functionals of $\varphi^{(q)}_{1k}(r)$ and $\varphi^{(q)}_{2k}(r)$ which are solutions of the Hartree-Fock-Bogoliubov equations

$$\begin{pmatrix} h_q(r) - \lambda_q & \Delta_q(r) \\ \Delta_q(r) & -h_q(r) + \lambda_q \end{pmatrix} \begin{pmatrix} \varphi^{(q)}_{1k}(r) \\ \varphi^{(q)}_{2k}(r) \end{pmatrix} = E^{(q)}_k \begin{pmatrix} \varphi^{(q)}_{1k}(r) \\ \varphi^{(q)}_{2k}(r) \end{pmatrix}$$

$$h_q \equiv -\boldsymbol{\nabla} \cdot \frac{\delta E}{\delta \tau_q}\boldsymbol{\nabla} + \frac{\delta E}{\delta \rho_q} - \mathrm{i}\frac{\delta E}{\delta \boldsymbol{J}_q} \cdot \boldsymbol{\nabla} \times \boldsymbol{\sigma}\,, \qquad \Delta_q \equiv \frac{\delta E}{\delta \tilde{\rho}_q}$$

Effective nuclear energy density functional

- **In principle, one can construct the nuclear functional from realistic NN forces** (i.e. fitted to experimental NN phase shifts) using many-body methods

$$\mathcal{E} = \frac{\hbar^2}{2M}(\tau_n + \tau_p) + A(\rho_n, \rho_p) + B(\rho_n, \rho_p)\tau_n + B(\rho_p, \rho_n)\tau_p$$

$$+C(\rho_n, \rho_p)(\nabla\rho_n)^2 + C(\rho_p, \rho_n)(\nabla\rho_p)^2 + D(\rho_n, \rho_p)(\nabla\rho_n)\cdot(\nabla\rho_p)$$

+ Coulomb, spin-orbit and pairing

Drut,Furnstahl and Platter,Prog.Part.Nucl.Phys.64(2010)120.

- **But this is a very difficult task** so in practice, we construct phenomenological (Skyrme) functionals
Bender,Heenen and Reinhard,Rev.Mod.Phys.75, 121 (2003).

Why not using existing Skyrme functionals?

There currently exists more than 100 Skyrme functionals. Why do we need more?

Most of these functionals are not suitable for astrophysics.

- They were adjusted to a few selected nuclei (mostly in the stability valley)
  $\rightarrow$ not suited for investigating stellar nucleosynthesis.
- They were not fitted to the neutron-matter EoS
  $\rightarrow$ not suited for neutron-star studies.

It is difficult to get physical insight on how to optimize the functional because each one was constructed using a different fitting procedure.

Construction of the functional

Experimental data:

- 2149 atomic masses with $Z, N \geq 8$ from 2003 AME
- compressibility $230 \leq K_v \leq 250$ MeV
- charge radius of ^{208}Pb, $R_c = 5.501 \pm 0.001$ fm
- symmetry energy $J = 30$ MeV

N-body calculations with realistic forces:

- isoscalar effective mass $M_s^*/M = 0.8$
- equation of state of pure neutron matter
- $^1S_0$ pairing gaps in symmetric and neutron matter
- Landau parameters, stability against spurious spin and spin-isospin instabilities

With these constraints, the functional is well suited for astrophysical applications.

Phenomenological corrections for atomic nuclei

For atomic nuclei, we add the following corrections not taken into account in Skyrme functionals:

- Wigner energy

$$E_W = V_W \exp\left\{-\lambda\left(\frac{N-Z}{A}\right)^2\right\} + V_W'|N-Z| \exp\left\{-\left(\frac{A}{A_0}\right)^2\right\}$$

- rotational and vibrational spurious collective energy

$$E_{\rm coll} = E_{\rm rot}^{\rm crank}\left\{b \ \tanh(c|\beta_2|) + d|\beta_2| \ \exp\{-l(|\beta_2| - \beta_2^0)^2\}\right\}$$

In this way, these collective effects do not contaminate the parameters of the functional.

Pairing functional

Empirical pairing energy density functionals

The pairing functional is generally parametrized as

$$\mathcal{E}_{\rm pair} = \frac{1}{4}\sum_{q=n,p} v^{\pi q}[\rho_n, \rho_p]\tilde{\rho}_q^2$$

$$v^{\pi q}[\rho_n, \rho_p] = V_{\pi q}^{\Lambda}\left(1 - \eta_q\left(\frac{\rho_n + \rho_p}{\rho_0}\right)^{\alpha_q}\right)$$

This functional has to be supplemented with a cutoff prescription.

Drawbacks

- not enough flexibility to fit realistic pairing gaps in infinite nuclear matter and in finite nuclei ($\Rightarrow$ isospin dependence)
- the global fit to nuclear masses would be computationally very expensive

Non-empirical pairing functional

Assumption:

$v^{\pi q}[\rho_n(\boldsymbol{r}), \rho_p(\boldsymbol{r})]$ is *locally* the same in nuclei as in homogeneous nuclear matter with densities $\rho_n(\boldsymbol{r})$ and $\rho_p(\boldsymbol{r})$

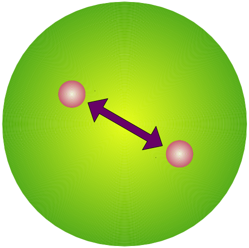

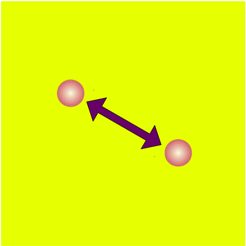

$v^{\pi q}[\rho_n, \rho_p] = v^{\pi q}[\Delta_q(\rho_n, \rho_p)]$ constructed so as to reproduce *exactly* a given pairing gap Δ_q in infinite homogeneous matter by solving *directly* the HFB equations

Chamel, Goriely, Pearson, Nucl. Phys.A812,72 (2008).

Pairing in nuclei and in nuclear matter

Inverting the HFB equations yields

$$v^{\pi q} = -8\pi^2 \left(\frac{\hbar^2}{2M_q^*}\right)^{3/2} \left(\int_0^{\mu_q+\varepsilon_\Lambda} \frac{\sqrt{\varepsilon}\mathrm{d}\varepsilon}{\sqrt{(\varepsilon-\mu_q)^2+\Delta_q(\rho_n,\rho_p)^2}}\right)^{-1}$$

$$\mu_q = \frac{\hbar^2}{2M_q^*}(3\pi^2\rho_q)^{2/3}$$

s.p. energy cutoff ε_Λ above the Fermi level

This procedure provides a **one-to-one correspondence between pairing in finite nuclei and pairing in homogneous nuclear matter**.

Analytical expression of the pairing strength

In the "weak-coupling approximation" $\Delta_q \ll \mu_q$ and $\Delta_q \ll \varepsilon_\Lambda$

$$v^{\pi q}[\rho_n, \rho_p] = -\frac{8\pi^2}{I_q(\rho_n, \rho_p)} \left(\frac{\hbar^2}{2M_q^*}\right)^{3/2}$$

$$I_q = \sqrt{\mu_q}\left[2\log\left(\frac{2\mu_q}{\Delta_q}\right) + \Lambda\left(\frac{\varepsilon_\Lambda}{\mu_q}\right)\right]$$

$$\Lambda(x) = \log(16x) + 2\sqrt{1+x} - 2\log\left(1+\sqrt{1+x}\right) - 4$$

Chamel, Phys. Rev. C 82, 014313 (2010)

- **exact fit** of the given gap function $\Delta_q(\rho_n, \rho_p)$
- **no free parameters**
- **automatic renormalization** of the pairing strength with ε_Λ

Pairing gaps from contact interactions

The weak-coupling approximation can also be used to determine the pairing gap of a Fermi gas interacting with a contact force

$$\Delta = 2\mu \exp\left(\frac{2}{g(\mu) v^{\pi}_{\mathrm{reg}}}\right)$$

μ is the chemical potential, $g(\mu)$ is the density of states and v^{π}_{reg} is a “regularized” interaction

$$\frac{1}{v^{\pi}_{\mathrm{reg}}} = \frac{1}{v^{\pi}} + \frac{1}{v^{\pi}_{\Lambda}}$$

$$v^{\pi}_{\Lambda} = \frac{4}{g(\mu)\Lambda(\varepsilon_{\Lambda}/\mu)}$$

Accuracy of the weak-coupling approximation

This approximation remains **very accurate at low densities** because the s.p. density of states is not replaced by a constant as in the usual “weak-coupling approximation”.
Example: HFB-17

symmetric nuclear matter

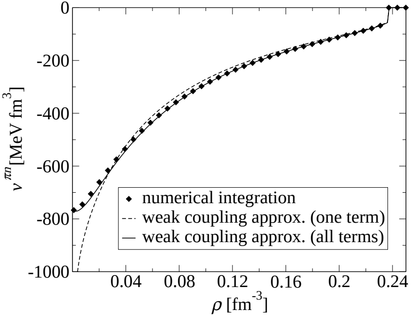

neutron matter

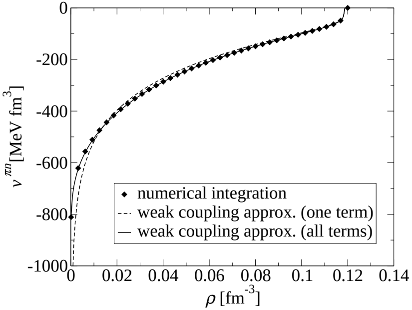

Chamel, Phys. Rev. C 82, 014313 (2010)

Accuracy of the weak-coupling approximation

This approximation remains **very accurate at low densities** because the s.p. density of states is not replaced by a constant as in the usual “weak-coupling approximation”.

Example: HFB-17

symmetric nuclear matter

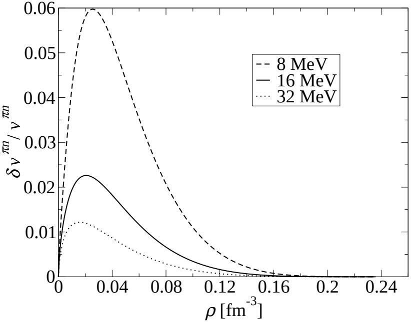

neutron matter

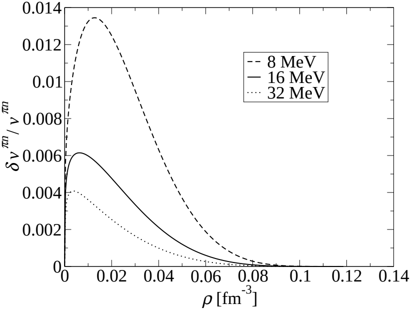

Chamel, Phys. Rev. C 82, 014313 (2010)

Pairing in dilute neutron matter

At very low densities, the pairing gap is given by

$$\Delta_n = \left(\frac{2}{e}\right)^{7/3} \mu_n \exp\left(\frac{\pi}{2k_{\mathrm{F}} a_{nn}}\right)$$

Gorkov&Melik-Barkhudarov, Sov. Phys. JETP, 13, 1018, (1961).

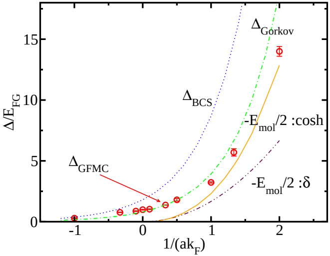

Chang et al. Phys.Rev.A70, 043602 (2004).

$$\Rightarrow v^{\pi n}[\rho_n] = -\frac{8\pi^2}{I_n(\rho_n)} \left(\frac{\hbar^2}{2M_n^*(\rho_n)}\right)^{3/2}$$

$$I_n = \sqrt{\mu_n}\left[\frac{14}{3} - \frac{8}{3}\log 2 - \left(\frac{\pi}{k_{\mathrm{F}} a_{nn}}\right) + \Lambda\left(\frac{\varepsilon_\Lambda}{\mu_n}\right)\right]$$

Pairing cutoff and experimental phase shifts

In the limit of vanishing density, the pairing strength

$$v^{\pi q}[\rho_q \to 0] = -\frac{4\pi^2}{\sqrt{\varepsilon_\Lambda}}\left(\frac{\hbar^2}{2M_q}\right)^{3/2}$$

should coincide with the bare force in the $^1S_0$ channel.

A fit to the **experimental $^1\mathbf{S}_0$ NN phase shifts** yields
$\varepsilon_\Lambda \sim 7 - 8$ MeV.
Esbensen et al., Phys. Rev. C 56, 3054 (1997).

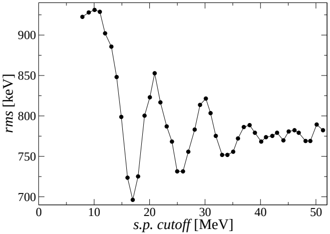

On the other hand, a better mass fit can be obtained with $\varepsilon_\Lambda \sim 16$ MeV while convergence is achieved for $\varepsilon_\Lambda \gtrsim 40$ MeV.
Goriely et al., Nucl.Phys.A773(2006),279.

Choice of the pairing gap

Fit the $^1S_0$ pairing gap obtained with realistic NN potentials at the BCS level

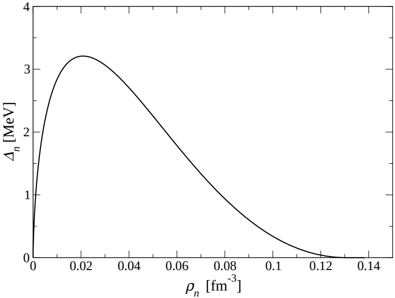

$^1S_0$ pairing gaps in neutron matter obtained with Argonne $V14$ potential

- $\Delta_n(\rho_n)$ essentially independent of the NN potential
- $\Delta_n(\rho_n)$ completely determined by experimental $^1S_0$ nn phase shifts

Dean&Hjorth-Jensen,Rev.Mod.Phys.75(2003)607.

Neutron vs proton pairing

With the microscopic BCS gaps, $v^{\pi q}[\rho_n, \rho_p] = v^{\pi}[\rho_q]$.

- Because of possible **charge symmetry breaking effects**, proton and neutron pairing strengths may not be equal

$$v^{\pi\, n}[\rho] \neq v^{\pi\, p}[\rho]$$

- The neglect of **polarization effects in odd nuclei** (equal filling approximation) is corrected by “staggered” pairing

$\Rightarrow$ we introduce renormalization factors $f_q^{\pm}$ ($f_n^{+} \equiv 1$ by definition)

$$v^{\pi\, n}[\rho_n] = f_n^{\pm} v^{\pi}[\rho_n]$$

$$v^{\pi\, p}[\rho_p] = f_p^{\pm} v^{\pi}[\rho_p]$$

Neutron vs proton pairing

What comes out of the global mass fit?

- neutron and proton pairing strengths are effectively equal
  $f_n^- / f_n^+ \simeq f_p^- / f_p^+$
- the pairing strength is larger for odd than for even nuclei
  $f_q^- \gtrsim f_q^+$

These results are consistent with the analysis of Bertsch, Bertulani, Nazarewicz, Schunck, Stoitsov, *Phys.Rev.C79(2009),034306*

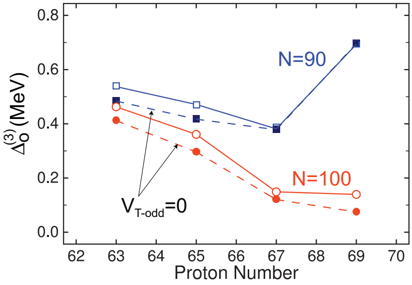

$^1S_0$ pairing gap in neutron matter

This new functional yields much more realistic pairing gaps than our previous functionals!

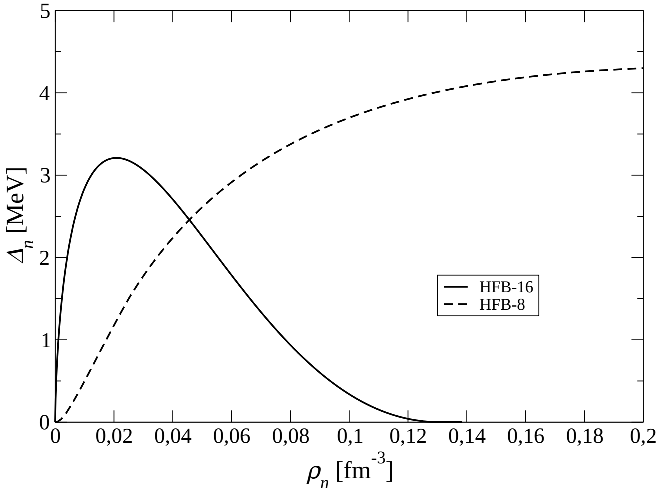

Neutron-matter equation of state

This functional is in very good agreement with realistic neutron-matter equations of state

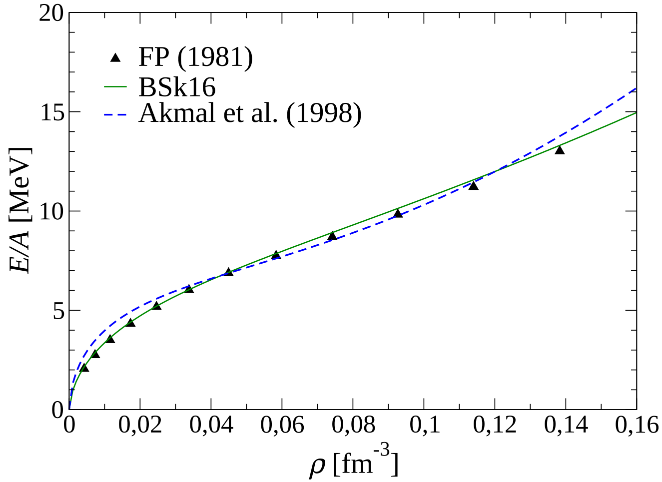

HFB-16 mass table

Results of the fit on the 2149 measured masses with $Z, N \geq 8$ from the 2003 Atomic Mass Evaluation

	HFB-16	FRDM
$\sigma(M)$ [MeV]	0.632	0.656
$\bar{\epsilon}(M)$ [MeV]	-0.001	0.058
$\sigma(M_{nr})$ [MeV]	0.748	0.919
$\bar{\epsilon}(M_{nr})$ [MeV]	0.161	0.047
$\sigma(S_n)$ [MeV]	0.500	0.399
$\bar{\epsilon}(S_n)$ [MeV]	-0.012	-0.001
$\sigma(Q_\beta)$ [MeV]	0.559	0.498
$\bar{\epsilon}(Q_\beta)$ [MeV]	0.031	0.004
$\sigma(R_c)$ [fm]	0.0313	0.0545
$\bar{\epsilon}(R_c)$ [fm]	-0.0149	-0.0366

Chamel, Goriely, Pearson, Nucl. Phys.A812,72 (2008).

Pairing predictions in nuclei

$N_0 = 50$ shell gap as function of Z for mass model HFB-16.

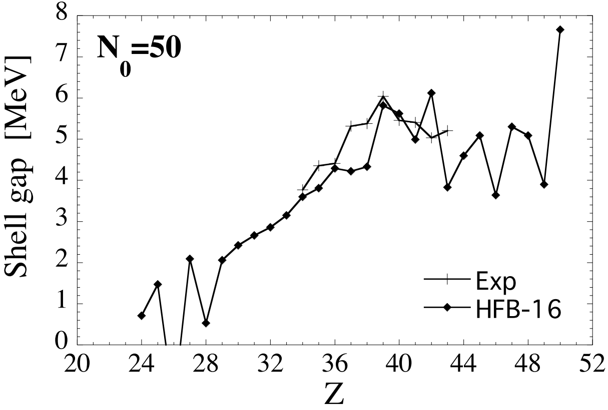

Chamel, Goriely, Pearson, Nucl. Phys.A812,72 (2008)

Pairing predictions in nuclei

$N_0 = 82$ shell gap as function of Z for mass model HFB-16.

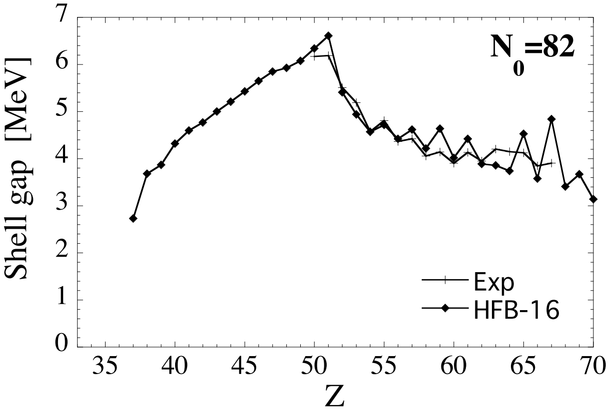

Chamel, Goriely, Pearson, Nucl. Phys.A812,72 (2008)

Pairing predictions in nuclei

$N_0 = 126$ shell gap as function of Z for mass model HFB-16.

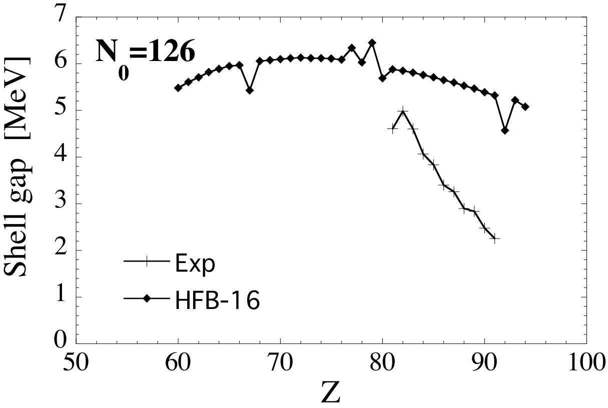

Chamel, Goriely, Pearson, Nucl. Phys.A812,72 (2008)

HFB-17 mass model: microscopic pairing gaps including medium polarization effects

Fit the $^1S_0$ pairing gaps of both neutron matter and symmetric nuclear matter obtained from **Brueckner calculations taking into account medium polarization effects**

Neutron matter

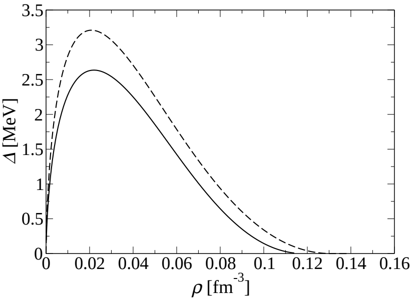

Symmetric nuclear matter

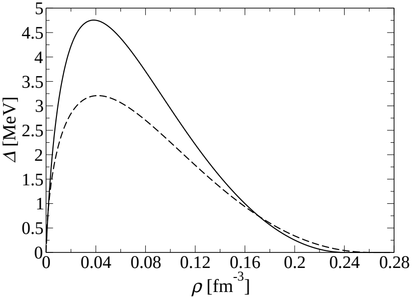

Cao et al.,Phys.Rev.C74,064301(2006).

New expression of the pairing strength

- the pairing strength now depends on both ρ_n and ρ_p

$$v^{\pi q}[\rho_n, \rho_p] = v^{\pi q}[\Delta_q(\rho_n, \rho_p)]$$

- $\Delta_q(\rho_n, \rho_p)$ is interpolated between that of symmetric matter (SM) and pure neutron matter (NM)

$$\Delta_q(\rho_n, \rho_p) = \Delta_{SM}(\rho)(1 - |\eta|) \pm \Delta_{NM}(\rho_q)\,\eta\,\frac{\rho_q}{\rho}$$

$$\eta = \frac{\rho_n - \rho_p}{\rho_n + \rho_p}$$

- $M_q^* = M$ to be consistent with the neglect of self-energy effects on the gap

Goriely, Chamel, Pearson, PRL102,152503 (2009).

Goriely, Chamel, Pearson, Eur.Phys.J.A42(2009),547.

Density dependence of the pairing strength

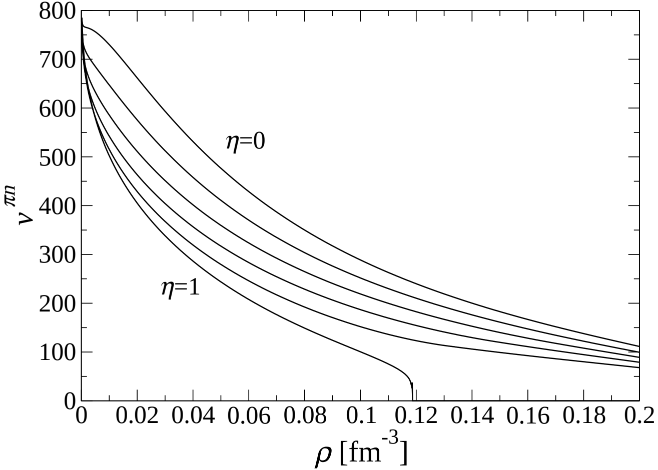

Isospin dependence of the pairing strength

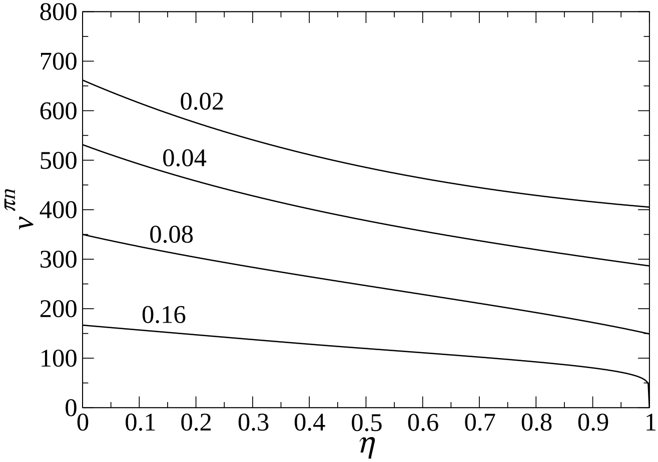

HFB-17 mass table

Results of the fit on the 2149 measured masses with $Z, N \geq 8$ from the 2003 Atomic Mass Evaluation

	HFB-16	HFB-17
$\sigma(2149\ M)$	**0.632**	**0.581**
$\bar{\epsilon}(2149\ M)$	-0.001	-0.019
$\sigma(M_{nr})$	0.748	0.729
$\bar{\epsilon}(M_{nr})$	0.161	0.119
$\sigma(S_n)$	0.500	0.506
$\bar{\epsilon}(S_n)$	-0.012	-0.010
$\sigma(Q_\beta)$	0.559	0.583
$\bar{\epsilon}(Q_\beta)$	0.031	0.022
$\sigma(R_c)$	0.0313	0.0300
$\bar{\epsilon}(R_c)$	-0.0149	-0.0114
$\theta(^{208}\mathrm{Pb})$	0.15	0.15

Goriely, Chamel, Pearson, PRL102,152503 (2009).

HFB-17 mass predictions

Differences between experimental and calculated masses as a function of the neutron number N for the HFB-17 mass model.

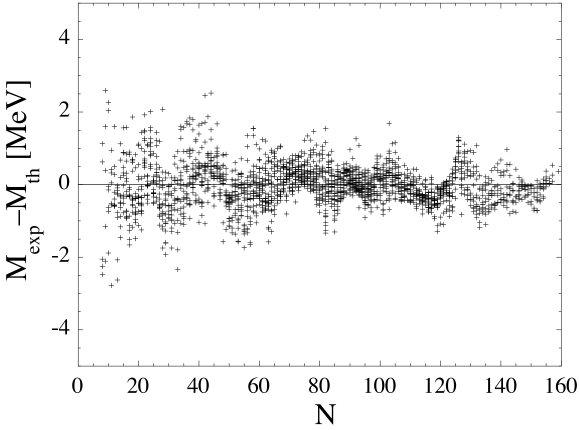

Goriely, Chamel, Pearson, PRL102,152503 (2009).

Nuclear masses: HFB-16 vs HFB-17

Differences between the HFB-16 and HFB-17 mass predictions as a function N for all $8 \leq Z \leq 110$ nuclei lying between the proton and neutron drip lines.

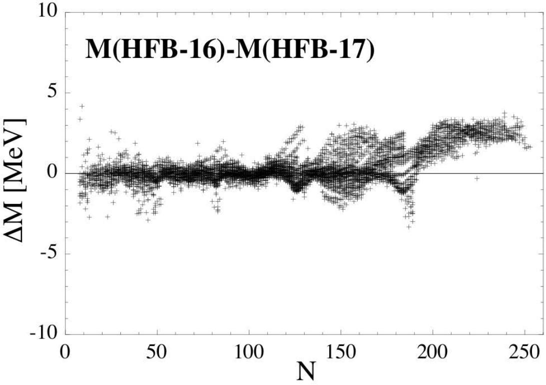

Nuclear matter properties BSk17 vs BSk16

	BSk16	BSk17
a_v	-16.053	-16.054
ρ_0	0.1586	0.1586
J	30.0	30.0
M_s^*/M	0.80	0.80
M_v^*/M	0.78	0.78
K_v	241.6	241.7
L	34.87	36.28

Note that both functionals lead to a splitting of effective masses that is qualitatively consistent with microscopic calculations.

Spin-isospin instabilities

Ferromagnetic instability

Unlike microscopic calculations, conventional Skyrme functionals predict a ferromagnetic transition in nuclear matter sometimes leading to a ferromagnetic collapse of neutron stars.

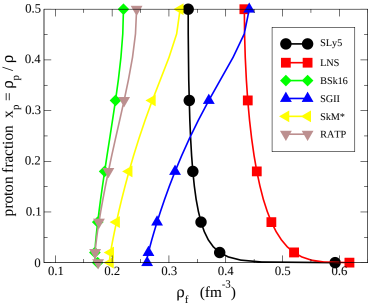

Margueron et al., J.Phys.G36(2009),125102.

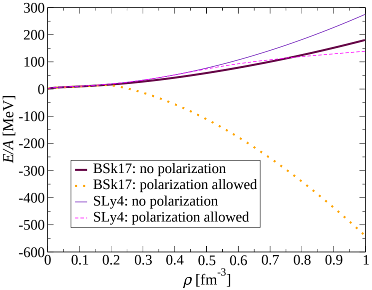

Chamel et al., Phys.Rev.C80(2009),065804.

Spin and spin-isospin instabilities

Skyrme functional in polarized homogeneous nuclear matter

$$\mathcal{E}^{\mathrm{pol}}_{\mathrm{Sky}} = \mathcal{E}^{\mathrm{unpol}}_{\mathrm{Sky}} + C_0^s \boldsymbol{s}^2 + C_1^s (\boldsymbol{s_n} - \boldsymbol{s_p})^2 + C_0^T \boldsymbol{s} \cdot \boldsymbol{T} + C_1^T (\boldsymbol{s_n} - \boldsymbol{s_p}) \cdot (\boldsymbol{T_n} - \boldsymbol{T_p})$$

with $s_q = \rho_{q\uparrow} - \rho_{q\downarrow}$ and $T_q = \tau_{q\uparrow} - \tau_{q\downarrow}$.

Spurious spin and spin-isospin instabilities arise from the C_0^T and C_1^T terms in the Skyrme functional.

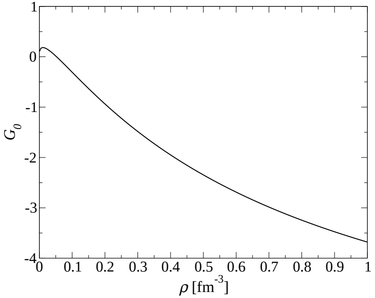

In symmetric nuclear matter, the ferromagnetic stability is governed by the Landau parameter $G_0 = 2N_0(C_0^s + C_0^T k_{\mathrm{F}}^2)$.

Spin stability in nuclear matter (partially) restored

The spurious ferromagnetic instability can be removed by including **spin density dependent** terms in the functional

In the framework of effective Skyrme forces, this can be achieved by adding new terms of the form ($\rho_s = s_n + s_p$, $\rho_{st} = s_n - s_p$)

$$\frac{1}{6} t_3^s (1 + x_3^s P_\sigma) \rho_s(\boldsymbol{r})^{\gamma_s} \delta(\boldsymbol{r}_{ij})$$

$$+ \frac{1}{6} t_3^{st} (1 + x_3^{st} P_\sigma) \rho_{st}(\boldsymbol{r})^{\gamma_{st}} \delta(\boldsymbol{r}_{ij})$$

Margueron & Sagawa, J.Phys.G36(2009),125102.

Spin stability in nuclear matter (partially) restored

The spin-dependent terms not only remove the ferromagnetic instability but also slightly improve the mass fit ($\sigma = 0.575$ MeV)

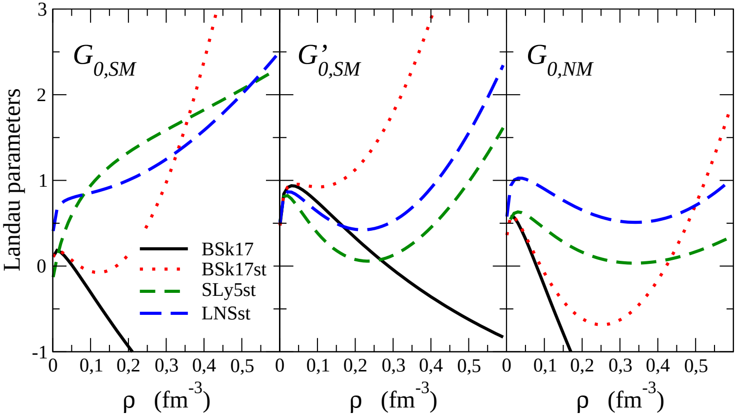

Margueron, Goriely, Grasso, Colò, Sagawa, J.Phys.G36(2009),125103.

Ferromagnetic transition at finite polarization

Problem: the new term removes the instability around $\delta_S \equiv (\rho_\uparrow - \rho_\downarrow)/\rho = 0$ but still predicts a ferromagnetic transition at finite $|\delta_S| > 0$

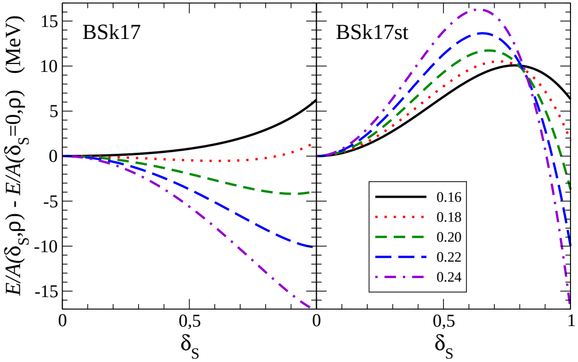

Margueron et al., J.Phys.G36(2009),125103.

Spin stability in symmetric nuclear matter restored

The ferromagnetic instability can be completely removed by including the **density-dependent** term in the Skyrme force

$$t_5(1+x_5P_\sigma)\frac{1}{\hbar^2}\boldsymbol{p}_{ij}.\rho(\boldsymbol{r})^\beta\,\delta(\boldsymbol{r}_{ij})\,\boldsymbol{p}_{ij}$$

Problem: this new term will also change the nuclear properties at low densities! Introduce another force of the form

$$\frac{1}{2}t_4(1+x_4P_\sigma)\frac{1}{\hbar^2}\left\{p_{ij}^2\,\rho(\boldsymbol{r})^\beta\,\delta(\boldsymbol{r}_{ij})+\delta(\boldsymbol{r}_{ij})\,\rho(\boldsymbol{r})^\beta\,p_{ij}^2\right\}$$

The t_4 and t_5 terms exactly cancel in unpolarized nuclear matter (for any isospin asymmetry) provided

$$t_4(1-x_4)=-3t_5(1+x_5),\; x_4(5+4x_5)=-(4+5x_5)$$

Chamel, Goriely, Pearson, Phys.Rev.C80(2009),065804.

Spin stability in asymmetric nuclear matter restored

With t_4 and t_5 terms, the ferromagnetic instability is completely removed not only in symmetric nuclear matter but also in neutron matter for any spin polarization.

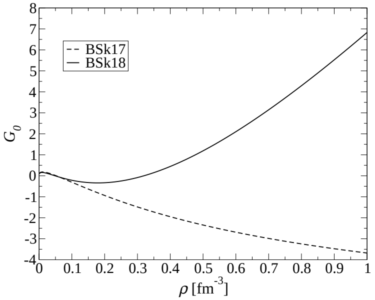

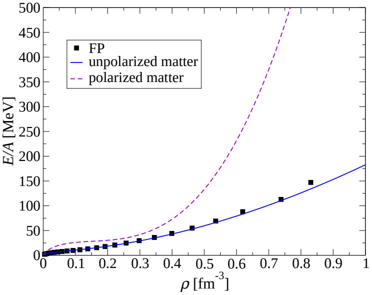

We have checked that no instabilities arise in neutron stars at any densities.

Chamel, Goriely, Pearson, Phys.Rev.C80(2009),065804.

HFB-18 mass model

Results of the fit on the 2149 measured masses with $Z, N \geq 8$

	HFB-18	HFB-17
$\sigma(M)$ [MeV]	0.585	0.581
$\bar{\epsilon}(M)$ [MeV]	0.007	-0.019
$\sigma(M_{nr})$ [MeV]	0.758	0.729
$\bar{\epsilon}(M_{nr})$ [MeV]	0.172	0.119
$\sigma(S_n)$ [MeV]	0.487	0.506
$\bar{\epsilon}(S_n)$ [MeV]	-0.012	-0.010
$\sigma(Q_\beta)$ [MeV]	0.561	0.583
$\bar{\epsilon}(Q_\beta)$ [MeV]	0.025	0.022
$\sigma(R_c)$ [fm]	0.0274	0.0300
$\bar{\epsilon}(R_c)$ [fm]	0.0016	-0.0114
$\theta(^{208}\mathrm{Pb})$ [fm]	0.15	0.15

$\Rightarrow$ HFB-18 yields almost identical results as HFB-17 for nuclei

Spin-isospin instabilities

Although HFB-18 yields stable neutron-star matter, it still predicts spurious spin-isospin instabilities in symmetric matter.

All instabilities (at any temperature and degree of polarization) can be removed by setting $C_t^T = 0$, which means dropping J^2 terms due to gauge invariance.

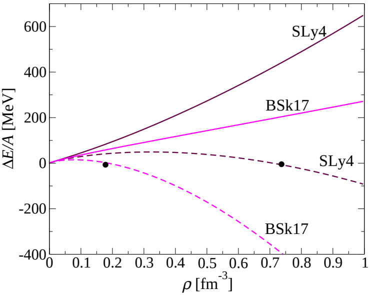

Difference between the energy per particle in fully polarized neutron matter and in unpolarized neutron matter with (dashed line) and without (solid line) C_t^T terms.
Chamel&Goriely, Phys.Rev.C82, 045804 (2010)

Landau parameters and the J^2 terms

Landau parameters for selected Skyrme forces which were fitted without the J^2 terms. Values in parenthesis were obtained by setting $C_t^T = 0$.

	G_0	G_0'	G_0^{NeuM}
SGII	0.01 (0.62)	0.51 (0.93)	-0.07 (1.19)
SLy4	1.11 (1.39)	-0.13 (0.90)	0.11 (1.27)
SkI1	-8.74 (1.09)	3.17 (0.90)	-5.57 (1.10)
SkI2	-1.18 (1.35)	0.77 (0.90)	-1.08 (1.24)
SkI3	0.57 (1.90)	0.20 (0.85)	-0.19 (1.35)
SkI4	-2.81 (1.77)	1.38 (0.88)	-2.03 (1.40)
SkI5	0.28 (1.79)	0.30 (0.85)	-0.31 (1.30)
SkO	-4.08 (0.48)	1.61 (0.98)	-3.17 (0.97)
LNS	0.83 (0.32)	0.14 (0.92)	0.59 (0.91)
Microscopic	0.83	1.22	0.77

Impact of the J^2 terms

Dropping the J^2 terms and their associated time-odd parts

- removes spin and spin-isospin instabilities at any $T \geq 0$
- prevents an anomalous behavior of the entropy
- improves the values of Landau parameters (especially G_0') and the sum rules.

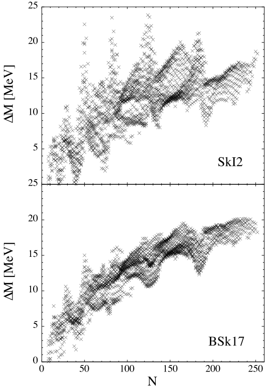

Warning:
Adding or removing a posteriori the J^2 terms without refitting the functional can induce large errors!

Chamel & Goriely, Phys.Rev.C82, 045804 (2010)

More about the J^2 terms

On the other hand dropping the J^2 terms leads to

- unrealistic effective masses in polarized matter

$$\frac{\hbar^2}{2M^*_{q\sigma}} = \frac{\hbar^2}{2M^*_q} \pm \left[s(C_0^T - C_1^T) + 2s_q C_1^T \right] \Rightarrow M^\star_{q\uparrow} = M^*_{q\downarrow} = M^*_q$$

- self-interaction errors.

Instabilities can be removed *with* the J^2 terms by adding density-dependent terms in C_0^T and C_1^T. But only for zero temperature.

Chamel, Goriely, Pearson, Phys.Rev.C80(2009),065804.

Self-interactions

Self-interactions

In the one-particle limit, the potential energy obtained from phenomenological functionals may not vanish.

Considering the most general semi-local functional with all possible bilinear terms up to 2nd order in the derivatives

$$\mathcal{E}_{\mathrm{Sky}} = \sum_{t=0,1} C_t^{\rho}\rho_t^2 + C_t^{\Delta\rho}\rho_t\Delta\rho_t + C_t^{\tau}\rho_t\tau_t + C_t^{\nabla J}\rho_t\nabla\cdot\boldsymbol{J_t}$$

$$+C_t^{J}\sum_{\mu,\nu}J_{t,\mu\nu}J_{t,\mu\nu} + \frac{1}{2}C_t^{TrJ}\left(\sum_{\mu}J_{t,\mu\mu}\right)^2 + \frac{1}{2}C_t^{J^2}\sum_{\mu,\nu}J_{t,\mu\nu}J_{t,\nu\mu}$$

$$+C_t^{s}s_t^2 + C_t^{\Delta s}\boldsymbol{s_t}\cdot\Delta\boldsymbol{s_t} + C_t^{T}\boldsymbol{s_t}\cdot\boldsymbol{T_t} + C_t^{j}j_t^2 + C_t^{\nabla j}\boldsymbol{s_t}\cdot\nabla\times\boldsymbol{j_t}$$

$$+C_t^{\nabla s}(\boldsymbol{\nabla}\cdot\boldsymbol{s_t})^2 + C_t^{F}\boldsymbol{s_t}\cdot\boldsymbol{F_t}$$

Removal of self-interactions

Requiring the cancellation of self-interactions leads to the fundamental constraints

$$C_0^{\rho} + C_1^{\rho} + C_0^{s} + C_1^{s} = 0$$

$$C_0^{\tau} + C_1^{\tau} + C_0^{T} + C_1^{T} = 4(C_0^{\Delta\rho} + C_1^{\Delta\rho} + C_0^{\Delta s} + C_1^{\Delta s})$$

$$4(C_0^{\nabla s} + C_1^{\nabla s}) + C_0^{F} + C_1^{F} = 0$$

$$C_0^{\tau} + C_1^{\tau} - 2(C_0^{T} + C_1^{T}) - (C_0^{F} + C_1^{F}) - 4(C_0^{\Delta s} + C_1^{\Delta s}) = 0$$

Chamel, Phys. Rev. C 82, 061307(R) (2010).

Self-interaction errors

Self-interaction errors in the one-particle limit can contaminate systems consisting of many particles.

For instance, in polarized neutron matter the error in the energy density caused by self-interactions is given by

$$\delta\mathcal{E}^{\mathrm{pol}}_{\mathrm{NeuM}} = (C^{\rho}_0 + C^{\rho}_1 + C^{s}_0 + C^{s}_1)\rho^2$$

If $C^{\rho}_0 + C^{\rho}_1 + C^{s}_0 + C^{s}_1 < 0$, self-interactions would thus drive a ferromagnetic collapse of neutron stars.

The use of effective forces prevent *one-particle* self-interaction errors but not necessarily *many-body* self-interaction errors (t_3 term).

Bender, Duguet and Lacroix, Phys. Rev. C 79, 044319 (2009).

Neutron-matter stiffness

Neutron-matter equation of state at high densities

We have recently constructed a family of three different generalized Skyrme functionals BSk19, BSk20 and BSk21 (with t_4 and t_5) spanning the range of realistic neutron-matter equations of state at high densities.

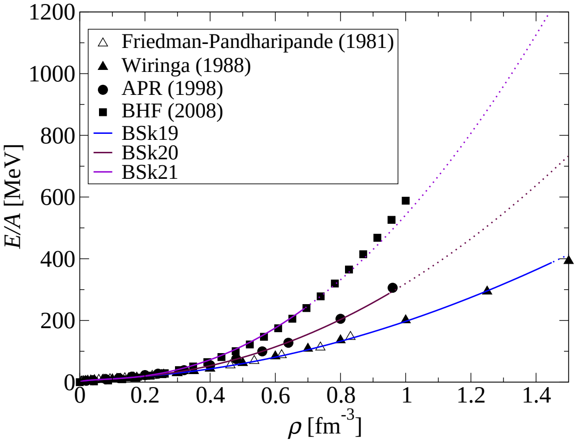

Neutron-matter equation of state at low densities

All three functionals yield similar neutron-matter equations of state at subsaturation densities consistent with microscopic calculations using realistic NN interactions

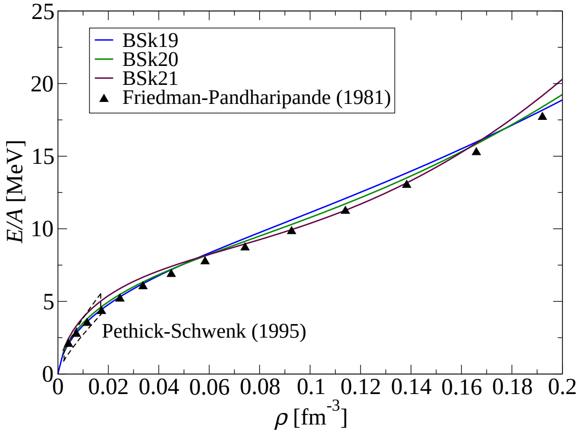

Nuclear-matter equation of state

Our functionals are also in very good agreement with BHF calculations not only in neutron matter but also in symmetric nuclear matter (not fitted).

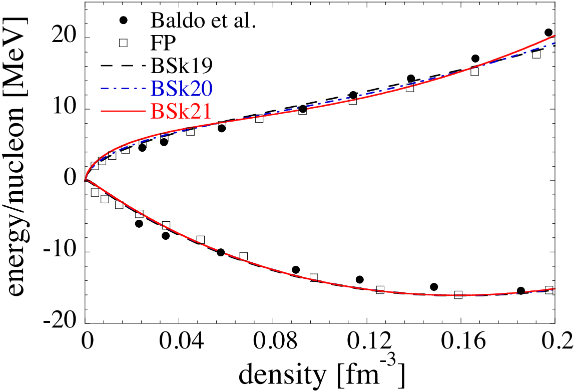

Constraints from heavy-ion collisions

Our functionals are consistent with the pressure of symmetric nuclear matter inferred from Au+Au collisions

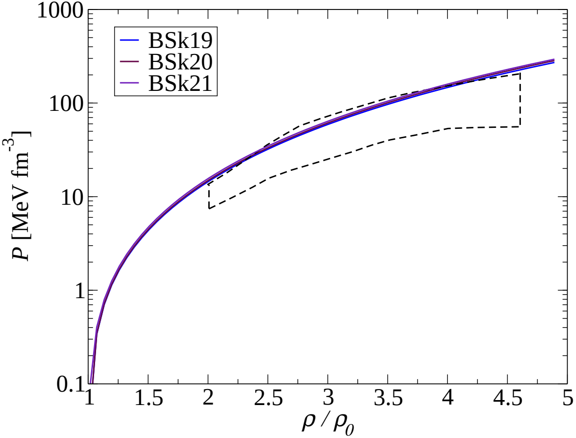

Danielewicz et al., Science 298, 1592 (2002).

HFB-19,HFB-20 and HFB-21 mass tables

Results of the fit on the 2149 measured masses with $Z, N \geq 8$ from the 2003 Atomic Mass Evaluation

	HFB-19	HFB-20	HFB-21	HFB-18
$\sigma(M)$ [MeV]	0.583	0.583	0.577	0.585
$\bar{\epsilon}(M)$ [MeV]	-0.038	0.021	-0.054	0.007
$\sigma(M_{nr})$ [MeV]	0.803	0.790	0.762	0.758
$\bar{\epsilon}(M_{nr})$ [MeV]	0.243	0.217	-0.086	0.172
$\sigma(S_n)$ [MeV]	0.502	0.525	0.532	0.487
$\bar{\epsilon}(S_n)$ [MeV]	-0.015	-0.012	-0.009	-0.012
$\sigma(Q_\beta)$ [MeV]	0.612	0.620	0.620	0.561
$\bar{\epsilon}(Q_\beta)$ [MeV]	0.027	0.024	0.000	0.025
$\sigma(R_c)$ [fm]	0.0283	0.0274	0.0270	0.0274
$\bar{\epsilon}(R_c)$ [fm]	-0.0032	0.0009	-0.0014	0.0016
$\theta(^{208}\text{Pb})$ [fm]	0.140	0.140	0.137	0.150

Goriely, Chamel, Pearson, Phys.Rev.C82,035804(2010).

Comparison with the latest experimental data

Comparison with the latest AME of 2294 nuclei transmitted by G. Audi (unpublished).

	$\bar{\epsilon}(M)$ [MeV]	$\sigma(M)$ [MeV]
HFB-21	-0.03092	0.5741786
HFB-20	-0.01002	0.5949311
HFB-19	0.05117	0.5934196
HFB-18	0.02584	0.5820830
HFB-17	0.0007729	0.5809776
FRDM	0.06163	0.6449888

Nuclear matter properties

	BSk19	BSk20	BSk21	BSk18
a_v [MeV]	-16.078	-16.080	-16.053	-16.063
ρ_0 [fm^{-3}]	0.1596	0.1596	0.1582	0.1586
J [MeV]	30.0	30.0	30.0	30.0
K_v [MeV]	237.3	241.4	245.8	241.8
L [MeV]	31.9	37.4	46.6	36.2
K_{sym}[MeV]	-191.4	-136.5	-37.2	-180.9
K_τ[MeV]	-342.8	-317.1	-264.6	-343.7
M_s^*/M	0.80	0.80	0.80	0.80
M_v^*/M	0.61	0.65	0.71	0.79

Note that BSk21 predicts a realistic splitting of effective masses in agreement with microscopic calculations.

Applications to neutron stars

Internal constitution of neutron stars

The interior of a neutron star contains **very different phases of matter**. A unified description of all regions of neutron stars is therefore very challenging.

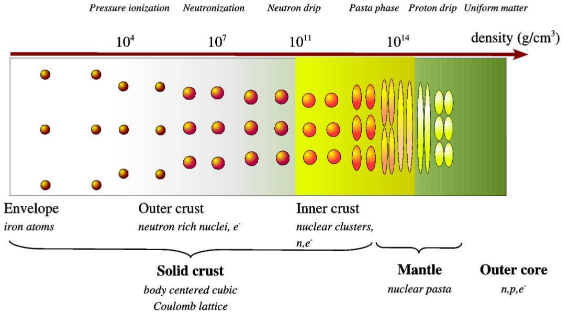

Chamel&Haensel, Living Reviews in Relativity 11 (2008), 10
http://relativity.livingreviews.org/Articles/lrr-2008-10/

Unified equation of state of a neutron star

The EDF theory allows for a unified treatment of all regions of a neutron star.

- **outer crust** (nuclei+relativistic electron gas)
  BPS model with HFB mass table
  Pearson, Goriely and Chamel,Phys.Rev.C 83,065810(2011).
- **inner crust** (clusters+neutron gas+relativistic electron gas)
  ETFSI+proton shell correction
  Onsi, Dutta, Chatri, Goriely, Chamel and Pearson,
  Phys.Rev.C77,065805 (2008).
  Pearson, Goriely, Chamel, Ducoin (2011).
- **core** (neutrons+protons+leptons)

Unified equation of state of neutron stars

All regions of neutron stars are described using the same functional.

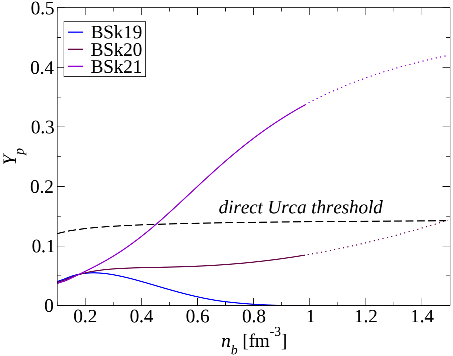

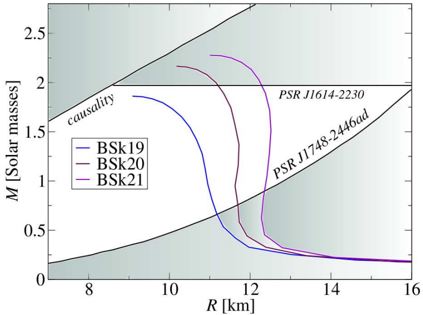

	n_{caus} (fm^{-3})	$\mathcal{M}_{max}/\mathcal{M}_\odot$	R (km)	n_{max} (fm^{-3})
BSk19	1.45	1.86 (1.84)	9.13	1.45
BSk20	0.98	2.14 (2.20)	10.6	0.98
BSk21	0.99	2.28 (2.3)	11.0	0.97

Summary

We have developed a family of Skyrme EDF constrained by both experiments and N-body calculations:

- they give an excellent fit to essentially all nuclear mass data ($\sigma \lesssim 0.6$ MeV)
- they give an excellent fit to other properties of finite nuclei such as charge radii ($\sigma \lesssim 0.03$ fm)
- they also reproduce various properties of homogeneous nuclear matter (EoS, pairing gaps, effective masses *etc*)
- they do not contain spurious instabilities in homogeneous nuclear matter (but spin-isospin part still needs to be improved)

With all these constraints, our EDF are well-suited for astrophysics.